



## SECTION 4

# GEOHERMAL POWER DEVELOPMENT IN OCEANIC AREAS

*Convenor :*

Dr. V. H. FORJAZ  
University of Lisbon  
Portugal



# PROJET DE SALINE A RIBEIRA GRANDE

by

GERARD ANDLAUER

Rue de Castelmau, Mundelsheim  
67450 France

## ABSTRACT

Le project consiste à capter l'eau chaude des sources de Furnas et à la canaliser jusqu'à proximité de Ribeira Quente ou seront disposés des bassins de saumure à l'air libre. L'eau chaude servira à élever la température de l'eau de mer de manière à obtenir une évaporation intense qui accélérera le dépôt du sel dissous. Celui-ci sera produit en quantité industrielle et à peu de frais. Il permettra de répondre à une forte demande locale sur le plan de l'agriculture et de la pêche.

*(This paper was not read at the Symposium)*



# GRAVITY RESIDUAL ANOMALIES AND GEOTHERMICS IN LATIUM REGION (CENTRAL ITALY)

by

M. DI FILIPPO\* and B. TORO\*\*

## ABSTRACT

Going from the thyrranian coast towards the Apennines (SW-NE), a general decrease in Bouguer anomaly values characterizes the Latium gravimetric field. This feature can be referred to a Moho progressive deepening. A sequence of higher order anomalies is superimposed on this back-ground (first order regional field); these higher order anomalies can be ascribed to thickness variations of a light cover (pyroclastics, shales, sands etc. with a density of 2.00-2.40) overlying a thick, mostly carbonatic basement havin ga density of 2.60-2.70 and forming the major geothermal reservoir. The analysis of the residual anomalies showed by a filtering of the first and second order regional fields ( $R = \sqrt{5}$  km) is very interesting when related generally to the geothermal phenomena and specifically

---

\* Istituto di Geologia e Paleontologia — Univ. — Roma

\*\* Centro di Studio per la Geologia dell'Italia Centrale CNR — Roma

to the known and supposed geothermal fields. From the n-1 residual anomalies map the following remarks appear: 1) Latium geothermal areas are located in residual gravimetric high zones and limited by gravimetric discontinuities, probably due to faults. 2) Latium known geothermal fields (Torre Alfina, Cesano, Latera) are located in residual gravimetric high zones. 3) The most productive wells are usually located on the edge of the gravimetric discontinuities. 4) The wells not productive because of permeability lack but having well bottom temperatures always high, are usually located in the upper portion of the structures.

Of remarkable interest concerning the other several Latium areas not yet explored but being on study; these areas occur in structural settlements similar to those of the known geothermal fields. Specifically we can notify:

- a) Tragliata structure and its southern extension
- b) Ciampino-Velletri structure (Albani Hills)
- c) Ardea and Anzio structures (SE of Rome).

The existence of high temperatures within these structures is not directly proved but can be strongly presumed by geochemical data and by analogies with close structures.

*(This paper was not read at the Symposium)*

# GEOLOGIC STRUCTURE AND FUMAROLIC ACTIVITY OF THE ESMERALDA SUBMARINE VOLCANO

by

A. P. GORSHKOV, G. M. GAVRILENKO,  
N. I. SELIVERSTOV and K. A. SCRIPKO

Institute of Volcanology,  
Petropavlovsk — Kamchatsky, 683006, USSR

## ABSTRACT

In 1978, geologic, geophysical and hydrochemical studies were conducted at the Esmeralda volcano onboard the R. V. Vulkanolog during cruises 4 and 5. These studies revealed submarine fumaroles on a slope of the crater at a depth of 80 m. Hydrochemical sampling of a train of submarine fumaroles with a series of water bottles showed the anomalously high concentrations of dissolved silicic acid and the lower chlorinity. Studies on the dynamics and chemical composition of the anomalous water layer permitted elaboration of a procedure for evaluation of the rate and phase state of heat transfer and of neat discharge of the volcano. In January 1978, the heat-transfer rate was at the minimum 1500 kg/s and the heat discharge was approximately  $(5-6) \times 10^5$  kcal/s; the heat transfer included approximately equal amounts of water and steam.

Native sulphur and other fumarolic products and hydrothermally altered rocks were recovered by dragging near the submarine fumaroles. Fresh ferromanganesian incrustations and nodules were discovered in the upper part of the cone.

Magmatic rocks are represented by aphyric and porphyric basalts, dolerite-basalts and gabbroids. Based on data of magnetic survey, the volcano is composed, mainly, of porphyric basalts. A sedimentary cover in the region of the Esmeralda volcano is represented exclusively by pyroclastic deposits. Their volumes were calculated using the results of seismic profiling. The main part of pyroclastic material is shown to be erupted and distributed in seawater.

## Part I

### FUMAROLIC ACTIVITY OF THE ESMERALDA VOLCANO IN JANUARY 1978 AND ITS QUANTITATIVE ESTIMATE

#### *Introduction*

The submarine Esmeralda volcano is located on the western submarine flank of the southern Mariana Island Arc 15 or 20 miles from Saipan and Tinian Islands. The first mention of this submarine volcano which was named «Esmeralda Bank» was made by Tanakadate (1940). This paper does not provide information on the activity of volcano, but gives only its coordinates (15°00'N, 145°16'E). In 1944 emission of gas bubbles with a sulphur dioxide odour was observed in this region (Hess, 1948). Based on this, Kuno (1962) included it to the «Catalogue of Active Volcanoes». On April 14, 1964, according to the U.S. Navy data, bursts of ash to a height of about 2400 m above sea level were observed in position 15°05'N, 145°08'E (Suwa, 1965). The Smithsonian Institution of the U.S.A. informed about its eruption on April 26 and 29, 1975 (Doubik and Litasova, 1978).



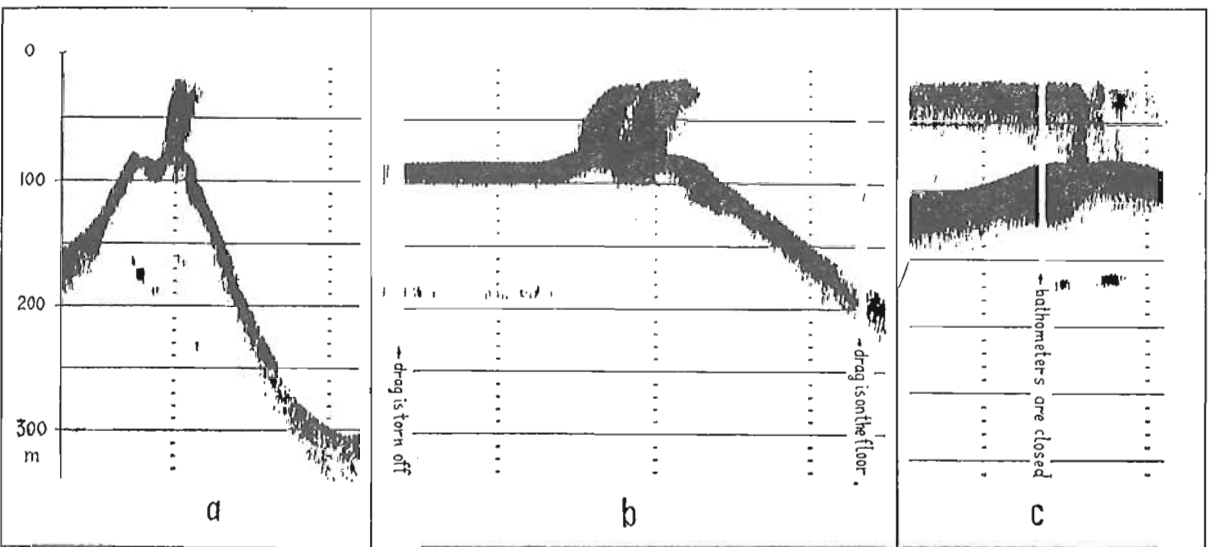


Fig. 1 — Example of submarine fumarole records on echograms, a — at a speed of 9.2 km/h. (echo sounding) ; b — at a speed of 2.3 km/h. (dragging) ; c — in drift (collection of water samples).

*Visual, Hydroacoustic and Hydrochemical Observations*

Submarine fumaroles fixed on echo sounding records as acoustic obstacles (Fig. 1) were detected on the northeastern rim of the crater at a depth of 80 m. Similar records were obtained earlier at other submarine volcanoes (Lavrov, 1966 ; Suwa and Ohura, 1975).

Cross dimensions of ascending flows of heated water saturated with gas bubbles were estimated to be from tens to hundreds of meters (Figs. 1, 2). Occasionally, a train of water with anomalous hydroacoustic and hydrochemical properties could be seen.

At the surface, the anomalous water train was distinguished by whitish, lime green colour. On January 18 and 19, 1978, two large isometric discoloured patches 0.3 and 0.4 km<sup>2</sup> in area were outlined. A lot of smaller patches and bands elongated with the stream were also observed. Within the patches of whitish colour we often observed small strongly outlined bright green and brown areas with emissions of gas bubbles, and perceived a slight sulphur dioxide odour. Suspension, collected from these areas, was determined to contain 0.2 ppm of iron.

Occasionally, the ascending flows did not reach the surface and their upper parts, like dense clouds of vapour, were seen at a depth of 5 to 10 m below sea level.

From January 14 to 20 the dimensions and position of discoloured patches changed continuously. Bursts of ash and gas, and fountains or columns of water were not recorded ; and solid silicate material was not found in water samples and in suspension.

Water samples for hydrochemical analyses were collected at 16 different sites, including 11 sites in the vicinity of the centre of activity within depth ranges from 0 to 220 m ; 4 sites on the flanks of submarine cone 1.5 miles (in radius) from the crater at depths of 600 to 900 m and 1 site 8.2 miles distant from the centre of activity at a depth of 2800 m. A total of

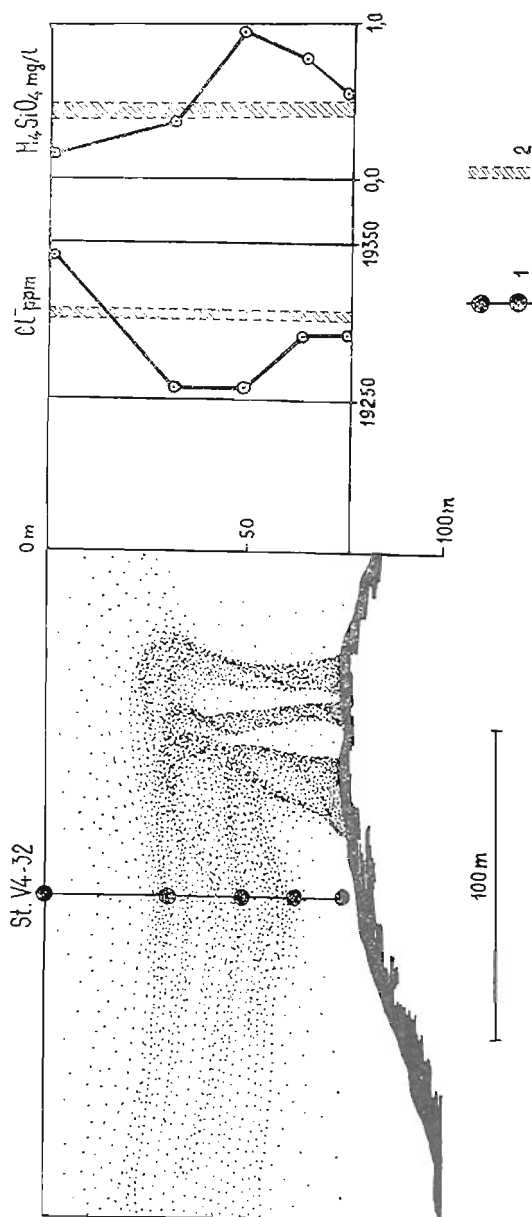


Fig. 2 — Variations in chloride-ion and dissolved silicic acid concentrations in seawater at site V4-32. 1 — water bottles, 2 — accuracy of component determination.

48 water samples was collected from the surface and at various depths, including 34 samples from the region of the crater. On each sample we measured pH values, total of halogens titrated with silver nitrate in recalculation to chloride ion concentration (chlorinity), and concentrations of dissolved silicic acid, sulphate ion and boric acid.

Data on changes in chlorinity and silica contents proved to be the most informative. Other components are not discussed in the present paper (see Gavrilenko et al., 1980). The chemical composition was seen to change mostly near the vents of fumaroles and in the train of anomalous seawater, implying the higher contents of dissolved silica and the lower chlorinity (see Fig. 2). These peculiarities of chemical composition permitted calculation of the amount of volcanic emanations supplied into seawater in the region of the crater and qualitative estimation of phase state of these volcanic emanations (deep heat transfer).

### *Estimation of Energy Parameters of Volcanic Activity*

#### 1. Fraction of Volcanic Component in the Anomalous Volume of Water

As chlorine ion is practically neutral in seawater, the observed hydrochemical lower chlorinity anomaly ( $Cl_{anom.}$ ) may be accounted for by dilution of seawater ( $Cl_{background}$ ) with volcanic emanations ( $Cl_{volc.}$ ).

In this case the fraction of volcanic component ( $N_{volc.}$ ) may be calculated from the formula of mixing (1), providing  $0 \leq Cl_{volc.} < Cl_{back.}$ , i.e. the chlorine ion concentration in volcanic emanations is too small in comparison to that in seawater. This agrees with data from other publications; besides, the

lower chlorinity anomalies in seawater near active submarine volcanoes were observed also earlier (Buljan, 1955; Sinyukov, 1964).

$$N_{\text{volc.}} = \frac{\text{Cl}_{\text{back.}} - \text{Cl}_{\text{anom.}}}{\text{Cl}_{\text{back.}} - \text{Cl}_{\text{volc.}}} \quad (1)$$

$\text{Cl}_{\text{back.}}$  and  $\text{Cl}_{\text{anom.}}$  were determined experimentally, 19 346 and 19 309.6 ppm, respectively ( $\text{Cl}_{\text{anom.}} = 19\,309.6 \pm 0.9$  ppm is the average of 29 samples with the accuracy of a single determination  $\pm 5$  ppm).

Assuming that  $\text{Cl}_{\text{volc.}} = 0$ , the minimum value for the fraction of volcanic component will be  $1.9 \times 10^{-3}$  or 0.19 %.

2. The deep heat-transfer rate ( $P_{\text{volc.}}$ ) was calculated from the formula :

$$P_{\text{volc.}} = N_{\text{volc.}} \cdot \rho \cdot b \cdot h \cdot v \quad (2)$$

where  $\rho$  is the density (1.03 ton/m<sup>3</sup>),  $b$  is the width of the anomalous water column (90 to 110 m),  $h$  is the depth (80 m) and  $v$  is the velocity of sea current;  $b$  and  $h$  were determined from echograms;  $v = 0.1$  m/ is the minimum velocity taken from the Atlas of Oceans ... (1974). Hence, the minimum value for the deep heat-transfer rate will be  $\sim 1500$  kg/s.

Similar results may be obtained by using another method of calculation. The volume of anomalous zone is  $(20 \text{ to } 30) \times 10^6$  m<sup>3</sup>. It contains  $\sim 5 \cdot 10^4$  m<sup>3</sup> of deep heat transferer (when  $N_{\text{volc.}} = 0.19$  %). The relaxation period of large anomalous zones, according to observations, is on the average 8 to 12 hours. Hence, the deep heat-transfer rate is approximately from 1100 to 1700 kg/s.

## 3. Temperature and Phase State of Deep Heat Transferrer

While dredging in the vicinity of fumaroles, the following low-temperature mineral aggregates were recovered: native sulphur, various sulphides, zeolites and hydromicaceous minerals. These minerals indicate a limited range of temperatures (120° to 250°C) of volcanic emanations near the vents of fumaroles. Since volcanic emanations consist mainly of water, the temperature of water boiling near the vents of fumaroles will be close to the temperature of pure water boiling, which is equal to 174.5°C under the pressure of 9 atm (80 m depth). Abundant native sulphur transferred with steam-gas fumarole jets indicate that at least part of volcanic emanations is represented by steam and gas jets whose temperature is above 175°C.

The following two types of hydrochemical zoning were distinguished at the anomalous sites: some sites show the decrease in chlorinity and increase in silica content and the other show the decrease in chlorinity only. (At these sites submarine fumaroles were also detected on echograms and bubbles of gas were observed.)

It is known that solubility of silica in vapour is some orders lower than in water at the same temperature. Therefore the mentioned differences may be accounted for by supply into seawater of thermal water transferring silica and of steam-gas mixture practically without silica. To be convinced of the correctness of this speculation, we calculated the contents of volcanogenic silica.

$$[\text{H}_4\text{SiO}_4]_{\text{volc.}} = \frac{[\text{H}_4\text{SiO}_4]_{\text{obs.}}}{N_{\text{volc.}}} = \frac{[\text{H}_4\text{SiO}_4]_{\text{obs.}}}{1 - \frac{\text{Cl}_{\text{obs.}}}{\text{Cl}_{\text{back.}}}} \quad (3)$$

On the basis of these calculations, the average silica content in fumarole jets for type I hydrochemical zoning is 160 to 210 mg/l. These values are similar to the silica contents in thermal waters of volcanic areas on land.

Thus, there is every reason to believe that the phase state of volcanic emanations is different and is represented by a steam-gas mixture with a temperature of above 175°C and by thermal waters with a temperature below 175°C.

Since samples with higher and background contents of dissolved silica in the region of the centre of volcanic activity were recovered in approximately equal amounts one can assume that the deep heat transferer is represented by approximately equal amounts (by mass) of vapour and liquid.

#### 4. Thermal Capacity of Volcano

Within the temperature ranges from 120 to 250°C the enthalpy of heat transferer may be from 120 to 700 kcal/kg (120.4 kcal/kg for water at temperature of 120°C and 703.2 kcal/kg for vapour with temperature of 250°C). Assuming that the amounts of water and vapour are equal and that the minimum value for the heat-transferer rate is 1500 kg/s, the heat discharge of volcano will be on the order of  $(5 \text{ to } 6) \times 10^5$  kcal/s.

Even with these minimal parameters of volcanic activity, the substance evacuation and energy of Esmeralda in January 1978 were compatible with those and even transcended the energy characteristics of the most active terrestrial volcanoes in Kamchatka during the period of interparoxysmal activity (Polyak, 1966; Kirsanova and Rozhkov, 1975; Gorshkov et al., 1972; 1975).

*Silicon and Iron Evacuation by Fumaroles*

The mentioned procedure of calculation of energy parameters allows us not only to compare the submarine volcanoes with the terrestrial ones, but also to estimate evacuation of some mineral components by submarine fumaroles. The average content of a component in the anomalous zone is  $1/N_{\text{volc.}}$  times less than that in the heat transferrer (volcanic emanations); in the given case it is approximately 500 times less. Knowing the heat-transferrer rate, we can calculate the specific evacuation of the component. Thus, according to representative samples, the evacuation of dissolved silica (in recalculation to  $\text{SiO}_2$ ) and iron was about 16 tons and 13 tons a day, respectively.

It is of importance that the mentioned values refer only to the period of intensification of submarine fumarolic activity which was observed in January, 1978. In July, 1978, during the next cruise of the R. V. Vulkanolog, the discoloured water patches and gas emissions were not observed above the crater.

## Part II

GEOLOGICAL STRUCTURE  
OF THE ESMERALDA VOLCANO

During two cruises we made complex geophysical profiles with a total length of 500 miles, and geologic sampling at 60 sites of which dredging at 42 sites. The position of sites of geological sampling was chosen using the results of geophysical investigations that allowed us to enhance the reliability of geological interpretation of geophysical data and describe all the main types of rocks (and partially their interrelationships), at the comparatively small number of sites.



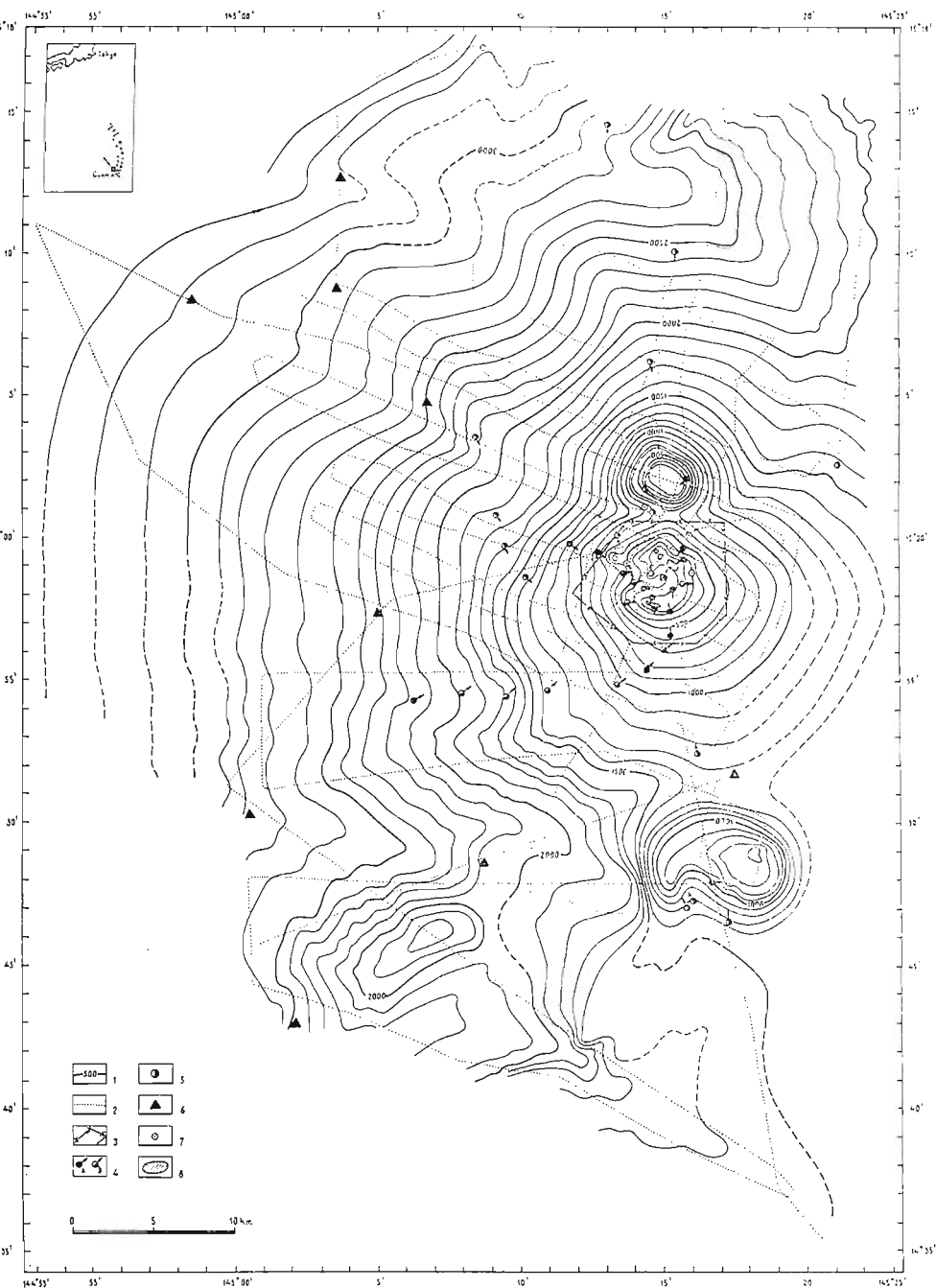


Fig. 3—Bathymetric map and scheme of site distribution of geologic and hydrochemical sampling of the Esmeralda volcano. 1—iso-baths; 2—tacks; 3—area of detailed investigations; 4-7—sites of sampling: 4—with a drag, a) from rock exposure, b) from piles, 5—with a ground tube, 6—with a dredge, 7—with water bottles; 8—zone of hydrochemical anomaly

### *Morphology of Volcanic Edifices*

On the bathymetric map (Fig. 3) one can recognize three isolated submarine mountains located submeridionally, parallel to the strike of the Mariana Arc. All of them are volcanic edifices. The northern and southern edifices are the extinct volcanoes covered partially by organic limestones. The central edifice is the active submarine Esmeralda volcano. It rises from a depth of 1500-2000 m; the diameter of its basement, by isobath 1500 m, is 15 to 20 km, the excess is approximately 1400 m. It differs from the Kamchatka terrestrial volcanoes similar in dimensions (Karymsky and Avachinsky) by more gentle slopes: 10 to 12° in the middle part and 15 to 18° in the upper part of the cone. At the top of the volcano there is a clearly expressed crater open westward. Its depth is about 300 m; the diameter by the crater rim is about 3 km, the upper crater rim is 50 to 100 m below sea level, and the minimum depth found on the northern crater rim is 43 m. On the northwestern slope of the cone one can distinguish local heights with an excess of from above ten meters to 100 m, interpreted as parasitic cones. On the northeastern crater rim we have found and investigated the submarine fumaroles which were described in Part I of the present paper.

### *Composition of Rocks*

Figures 4 and 5 show the geological (lithological-facial) scheme of the Esmeralda volcano constructed on the basis of geologic and geophysical data.

Magmatic rocks are represented by aphyric and porphyric basalts, dolerite-basalts and gabbroids. (The petrographic description of these rocks is given in more detail in Gorshkov et al., 1980).

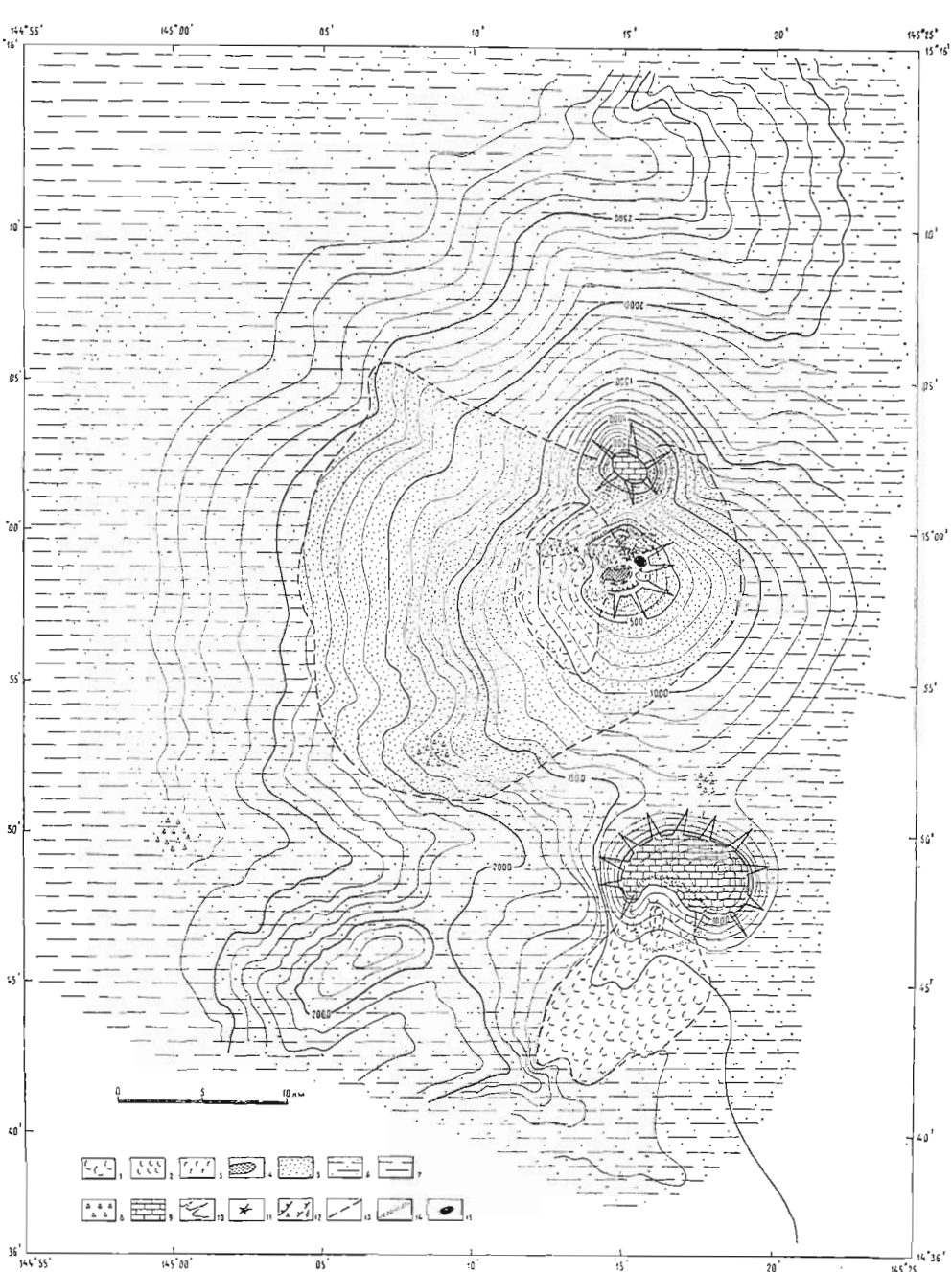


Fig. 4 — Lithological-facial scheme of the Esmeralda Volcano. 1 — andesite-basalts from the central cone; 2 — andesite-basalts from the young parasitic cones; 3 — gabbroid rocks; 4 — intercrateric deposits (tuffs, tufaceous sandstones, tufaceous gritstones, altered basalts and their scoriae); 5 — large-fragmental volcanoclastic material (bombs, scoria and lapilli); 6 — mid- and fine-fragmental material (volcanic sand and ash); 7 — aleuropelitic and pelitic oozes; 8 — pumice; 9 — organic limestones; 10 — volcanic edifices of the central type; 11 — parasitic cones:

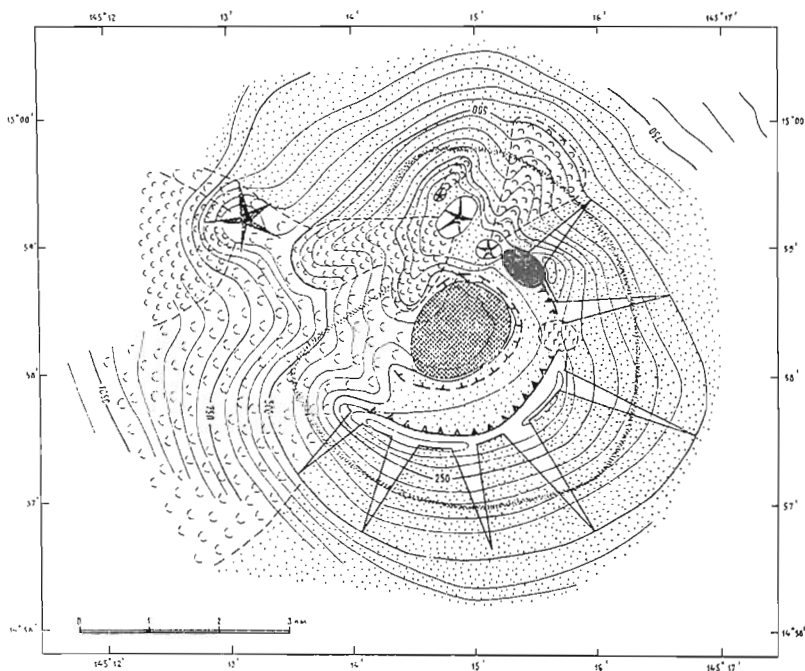


Fig. 5 — Structure of the crater and upper part of the cone. Symbols are as in Fig. 4.

It is to be noted that all types of magmatic rocks from glassy basalts to holocrystalline gabbroids were found spatially together. They were recovered in the same drag at depths from 140 m to 80 m. This fact along with their similar chemical composition give grounds for suggesting that all the mentioned rock varieties are derivatives of the same basaltic magma.

The sedimentary cover is represented exclusively by pyroclastic deposits. Large fragmental material (scoria, lapilli and volcanic bombs) is bordered by mid- and fine-fragmental material (volcanic sand and ash). The first sedimentary deposits (pelitic and aleuropelitic oozes) appear only at a distance of

30 to 35 km. Their thickness does not exceed a few centimetres. Below we find the pyroclastic material of the Esmeralda volcano.

Intracrateric deposits (see Fig. 5) are represented by tuffs, tufaceous sandstones, tufaceous gritstones and altered basalts and their scoriae.

A fumarolic field was discovered on the crater rim. While dragging, the following products of fumarolic activity were recovered; native sulphur, gypsum, opalite, alunite, iron hydroxides and sulphides.

Hydrothermally-altered rocks are distributed more widely. Alteration is developed mainly upon gabbroids and is manifested as chloritization, silicification and zeolitization. Geothite and limonite films are often found on the surface of samples. Hydro-micas and sulphides of secondary origin are also widely distributed.

Ferromanganesian formations occur everywhere on the volcanic edifice at depths from 80 m to 2500 m (Fig. 6). In most cases they differ strongly from incrustations and nodules which are indicative of oceanic depths. More often they occur as illinites and incrustations on the fragments of effusive rocks as well as cohere tufaceous sandstones and tufaceous gritstones. Their contents of iron range from 1.2 to 18.5 %, and of manganese from 0.2 to 42.8 %.

The Mn/Fe ratio varies from 0.02 to 32. One can see a clear tendency of Mn/Fe increasing with distance away from the active crater of volcano. These data along with the mentioned anomalous iron contents in suspension indicate that the active volcano is the main supplier of ore elements in this region. As for the Esmeralda volcano, metals are evacuated here by volcanic exhalations and hydrothermal solutions during the period of fumarolic activity. The intensity of iron evacuation, as it was shown previously in part I, was estimated to be 13 ton/day.

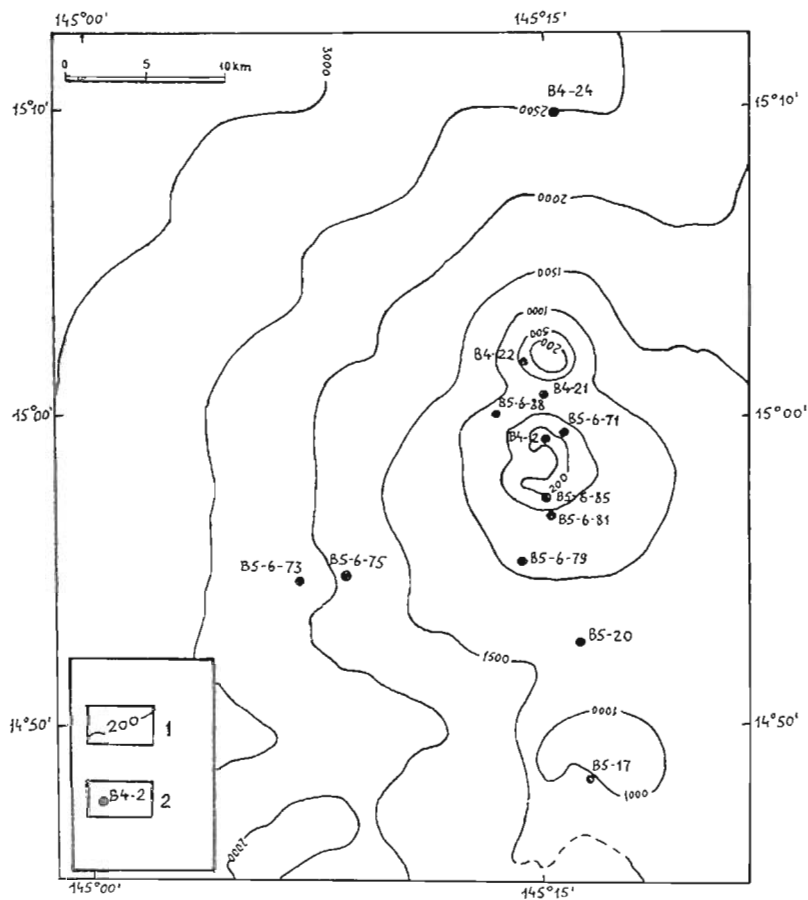


Fig. 6 — Scheme of site distribution with occurrences of ferromanganesian formations. 1 — isobaths ; 2 — site and its number.

TABLE 1

PHYSICAL PROPERTIES OF ROCKS RECOVERED IN THE REGION  
OF ESMERALDA VOLCANO

Rocks	Number of samples	Density $\delta$ g/cm <sup>3</sup>		Remanent magneti- zation $I_n$ A/m		Susceptibility $\kappa$ 10 <sup>-3</sup>	
		Variation	Average value	Variation	Average value	Variation	Average value
Porphyric andesite-basalts	3	1.88-2.35	2.04	2.2-6.8	4.7	0.2-6.8	4.0
Porphyric basalts	10	1.66-2.19	1.95	1.1-88.3	14.6	0.1-25.1	3.6
Leucogabbro	3	2.40-2.68	2.51	9.2-11.8	10.4	11.7-12.7	12.1
Scoriaceous, fine-porous aphyric basalts	8	1.51-2.40	1.81	24.3-71.5	40.2	0.8-11.3	2.6
Monolithic aphyric basalts with glassy crust	5	2.27-2.45	2.37	54-199	135	1.3-4.6	28.8
Altered aphyric basalts	3	1.98-2.21	2.06	1.5-2.2	1.9	1.6-15.3	6.1
Tufaceous sandstones	3	1.67-2.36	1.91	0.16-0.34	0.24	0.-280.52	0.4
Organic limestones	2	2.09-2.10	2.09	0.01-0.13	0.07	0.05-0.16	0.1

*Structure of Volcano According to Data  
of Hydromagnetic Survey*

According to data of geologic sampling, the Esmeralda volcano is composed mainly of basic rocks, including aphyric and porphyric basalts, gabbroids and intermediate dolerite-basalts. The altered rocks and newly-formed fumarolic mineral aggregates occur within the crater and upper part of the cone. However, as only slopes are accessible for sampling, a problem arises whether or not the recovered samples are typical of the volcano as a whole or what is the inner structure of the volcano.

To respond partially these questions, data of magnetic survey and studies on physical properties of samples may be used.

The magnetic field from volcano is represented by anomalies of two signs having the total intensity of up to 1000 nT and complicating local anomalies tending to occur within the crater and upper part of the edifice (Fig. 7). The presence of positive and negative parts of anomaly from the cone may be explained by the fact that for the given latitude the angle of normal inclination of total vector  $T$  is  $15^\circ$ . In this case the objects magnetized by recent magnetic field will create anomalies of two signs approximately of equal amplitudes similar to a source with horizontal magnetization.

In terms of magnetic properties the rocks from the Esmeralda volcano are strongly differentiated (Table). The mean values for remanent magnetization of porphyric basalts are within the range of (5 to 15) A/m. The remanent magnetization of aphyric basalts is by an order higher than that of porphyric basalts. Gabbroids do not differ in remanent magnetization from porphyric basalts. Altered basalt varieties are slightly magnetized and tufaceous sandstones and organic rocks are practically non-magnetic.



# SYMPOSIUM ON THE ACTIVITY OF OCEANIC VOLCANOES

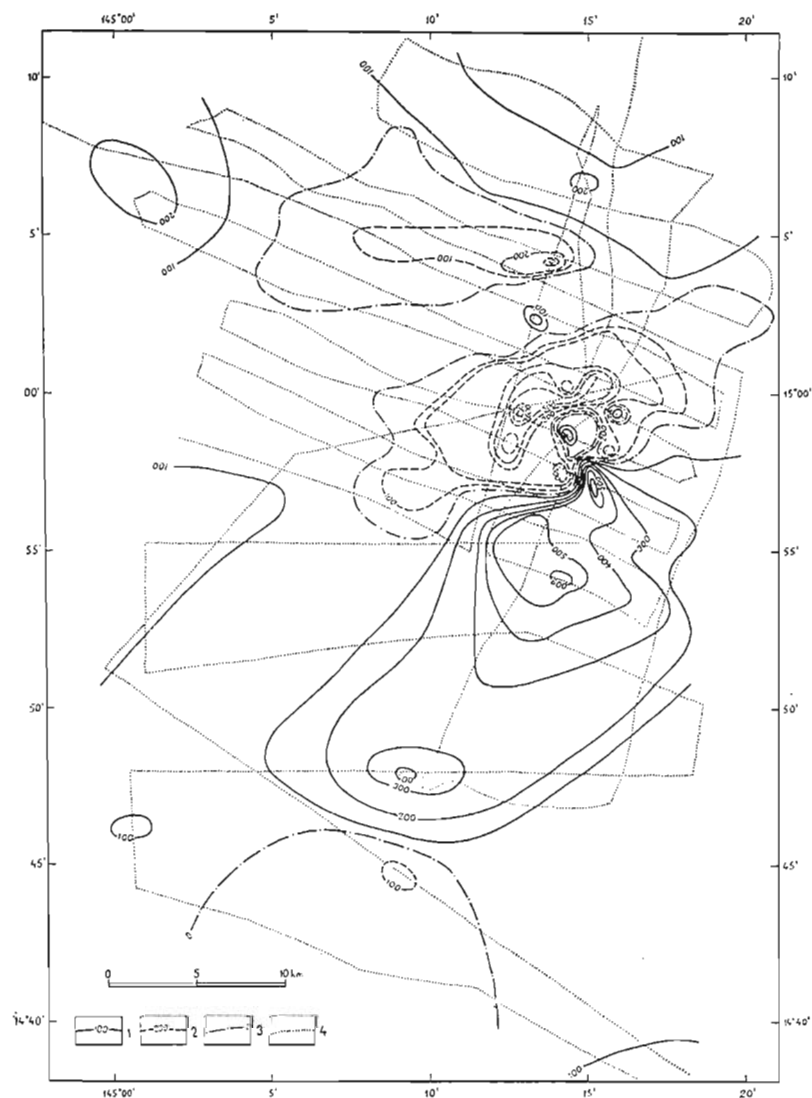


Fig. 7—Scheme of anomalous magnetic field of the Esmeralda volcano.  
1-3—isolines (in nT): 1—positive; 2—negative; 3—zero;  
4—tracks.

For the Esmeralda volcano the effective magnetization was calculated by solution of models with symmetrical bodies which were used for approximation of its edifice (Simonovsky and Kaminsky, 1975). An example of calculation is shown in Fig. 8 where the edifice was approximated by a combination of two truncated cones. A few variants of similar calculations resulted in the values for effective magnetization, 5 to 8 A/m. Thus, the average magnetization of the edifice responds, most of all, to porphyric basalts and gabbroids.

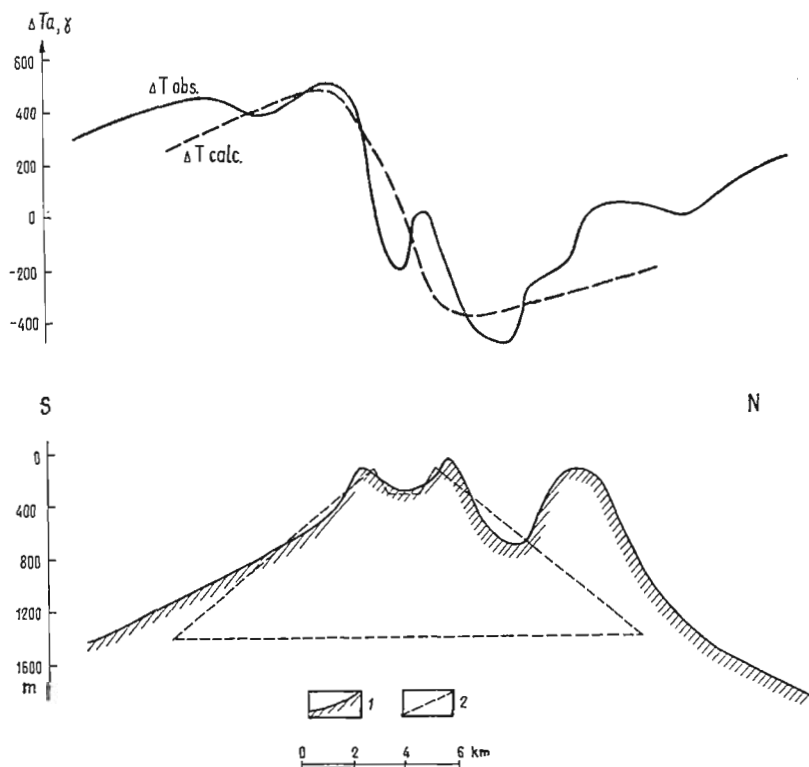


Fig. 8 — Calculated and observed magnetic field from the Esmeralda volcano along the meridional profile. 1 — topography of the edifice; 2 — model of the volcano approximated by the combination of two truncated cones with effective magnetization.  $I_{eff.} = 6$  A/m.

Based on this, we may propose that the volcano is composed predominantly of porphyric basalts. Aphyric basalts, having anomalously high magnetization, are characteristic only of the latest eruptions of the volcano. They produce local magnetic anomalies complicating the anomaly from the cone; their participation in the common section of the edifice is negligible.

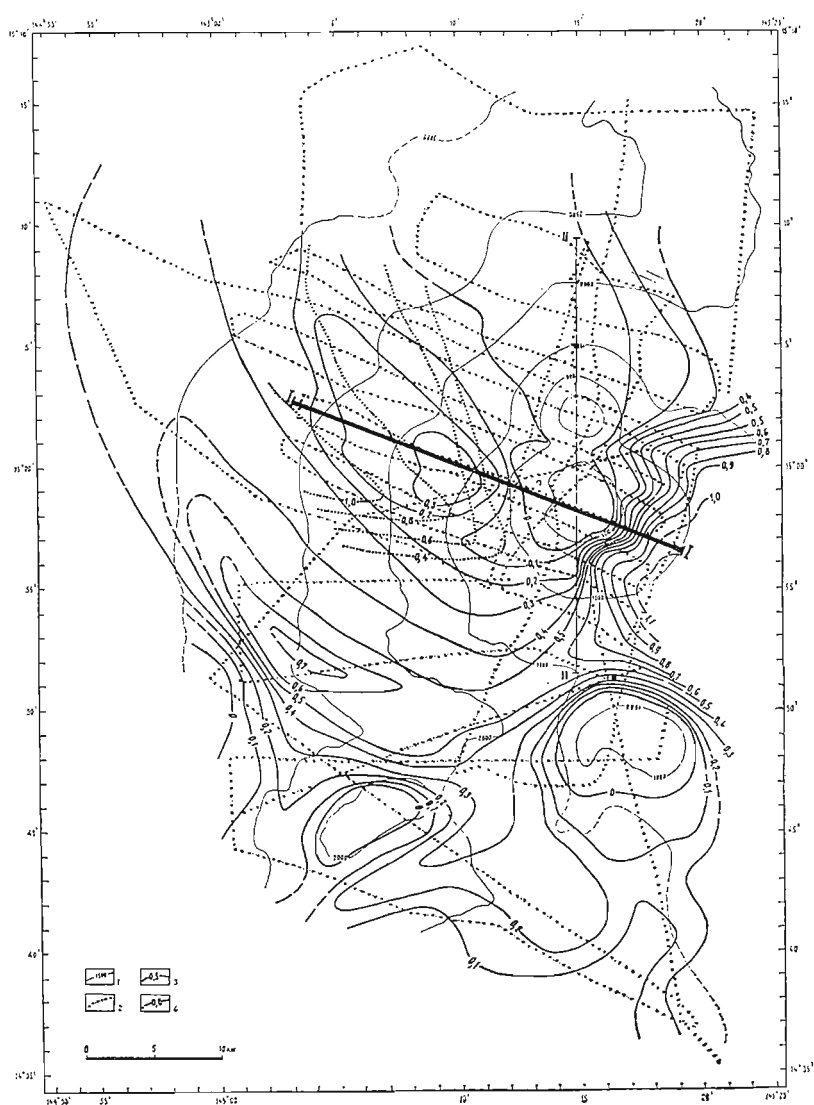
### *Composition and Structure of Sedimentary Cover*

A continuous seismic profiling (CSP) accomplished by a method of central ray with sparker along with data of geological sampling permitted us to construct a scheme of thicknesses of volcanogenic deposits (Fig. 9) and estimate scales of explosive and partly effusive activity of the volcano.

According to the CSP data, at the Esmeralda volcano the following two main types of wave pictures were distinguished: reflections from the surfaces of the acoustic type basement and reflections inside the stratum of «loose» deposits underlain by acoustic basement.

High intensity, interference composition, long duration and low correlativity are characteristic of the reflections from the surface of the acoustic type basement. The acoustic basement is exposed in the upper part and on the northern slope of the volcano (see Fig. 9). Dredging of these areas implied the presence of porphyric andesite-basalts. Based on this, the seismically rough records of reflections from the acoustic basement were interpreted as a roof of lava flows.

The intensity of reflections from the acoustic basement significantly decreases with the increasing thickness of upper-lying «loose» strata that is likely related to the formation of the transitional layer. Due to this effect, on the western flank of volcano one may distinguish reflections from deeper seismically rough boundaries of the acoustic basement type. They lie subparallel to the upper boundary (Fig. 10) and are inter-



preted as the surfaces of lava sheets the formation of which is likely associated with significant stages of effusive activity in the history of geological development of volcano.

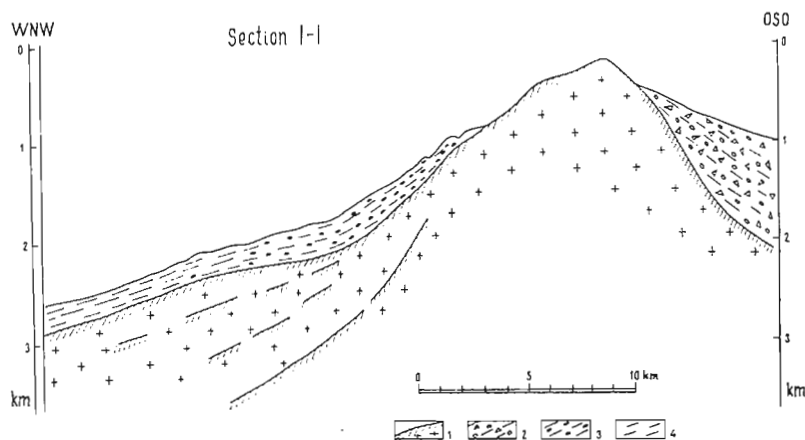


Fig. 10 — Section of the volcano along the sublatitudinal profile (I-I in Fig. 9), according to the CSP data. 1 — surface of acoustic basement (lava flows and sheets predominantly of porphyric basalts); 2-4 — pyroclastic material: 2 — predominantly large-fragmental; 3 — mid-; 4 — fine-fragmental. While constructing the section, the following seismic wave velocities were accepted: 5 km/s for 1; 2 km/s for 2-4.

While analysing the wave picture on the records of «loose» deposits and the scheme of thicknesses of these deposits, it was taken into account that the sedimentary cover in the volcano region was represented exclusively by pyroclastic deposits. All the fragmental material has an acute-angled shape without indications of roundness. The mineralogic composition of pyroclastics and fragmental material corresponds to the composition of basalts and gabbroids. Exceptions are the rare pumices of acid composition found only along hollows which may be brought with the stream from the Mariana islands.

The peculiarities of wave picture of «loose» deposits and the character of changes in their thicknesses may indicate that the entire section of sedimentary cover is composed of volcanogenic material. Exceptions are the deposits on the eastern flank of the volcano. Its section, on the basis of the CSP data, may contain both volcanogenic and terrigenous deposits. The latter may be brought from the Mariana islands (Gorshkov et al., 1980).

The thickness of pyroclastic deposits is from a few hundreds of meters on the southern flank to 1 km on the eastern flank (when the velocity of seismic waves  $V = 2 \text{ km/s}$ ). A bench of denser rocks, presumably, lava sheets with a thickness of up to 0.6 s (1.5 km when  $V = 5 \text{ km/s}$ ) lie on the western flank beneath strata of pyroclastic rocks. The structure of this area in section is shown in Fig. 10.

The total volume of the Esmeralda volcanogenic products is rather significant: not less than  $500 \text{ km}^3$  of pyroclastics and not less than  $300 \text{ km}^3$  of lava. It is to be noted that the mentioned value for pyroclastics is minimum, because measurements were made only within the edifice of the volcano. Really far beyond its edifice, 40 miles from the crater, one bottom core recovered only 20 cm of ooze below which lies pyroclastic material of the same composition that is characteristic of the Esmeralda magmatic rocks.

The character of changes in thicknesses indicates that the source of supply of both lava and pyroclastic material is the Esmeralda volcano. The absence of «loose» deposits in the north is notable. The extinct volcano, located to the north of the Esmeralda volcano, like a screen, prevents from migration of the pyroclastic material to the north. Analogous pictures may be seen at other heights surrounding the Esmeralda volcano. These facts may evidence that fragmental material spreads in seawater. It is supported also by findings of scoriae covered with glassy incrustations.

## CONCLUSIONS

Esmeralda is a large submarine volcano composed of basic rocks, porphyric basalts predominantly. Numerous samples of gabbroids found in the crater and upper part of the cone seem to indicate that on the bottom and walls of the crater a solidified channel is exposed. The Esmeralda volcano is similar in character of the erupted material distribution, morphology and internal structure to terrestrial volcanoes of the central type.

At present two main stages can be distinguished in the geologic history of the volcano: the first one, predominantly effusive, is characterized by the formation of the edifice and lava sheets with the thickness of up to 1.5 km on the western slope; the second one, predominantly explosive, is characterized by the formation of a thick sedimentary-pyroclastic cover with an area of a few thousands of km<sup>2</sup>.

It is to be noted that the Esmeralda volcanic activity is characterized by exceptionally large size and intensity, compared to other submarine island arc volcanoes. The total volume of ejected volcanic products is not less than 300 km<sup>3</sup> of lava and not less than 500 km<sup>3</sup> of pyroclastics. Explosive activity of the Esmeralda volcano is so vigorous that the processes of terrigenous and biogenic sedimentation are suppressed within the radius of many tens of kilometers. The main part of pyroclastic material covering the slopes and the foot of the volcano was erupted and spread in seawater. Inclusions of altered rocks in fresh basalts indicate the occurrence of gas-hydrothermal activity in the intervals between explosive eruptions.

In 1978, the intermittent submarine fumarolic activity and formation of altered rocks and newly-formed fumarolic mineral aggregates occurred at the Esmeralda volcano. For the first time the state of activity of submarine volcano was evaluated quantitatively. According to estimations, in January 1978, the

rate of heat transferrer (vapour and thermal waters) was not less than 1500 kg/s and the heat discharge was not less than  $(5 \text{ to } 6) \times 10^5$  kcal/s. The heat-transferrer consisted of approximately equal amounts of water and vapour.

It has been established that along with heat-transferrer silica ( $\sim 16$  tons/day) and iron (13 tons/day) were supplied into seawater.

It has also been established that ferromanganesian formations are formed on the slopes of the volcano as a result of fumarolic activity.



## REFERENCES

- Atlas of the Oceans. The Pacific Ocean.* 1974 GUN and O MO SSSR, 302 pp. charts (in Russian).
- BULJAN, M., 1955 : Deep submarine volcanism and the chemistry of ocean. Bull. Volcanol., Ser. II, T. 17, p. 41-56.
- DOUBIK, Yu. M. and LITASOVA, S. N., 1978 : Activity of the volcanoes of the world in 1975-1976 (according to data of the Smithsonian Institute). Bull. Volc. St., No. 55, p. 158-163 (in Russian).
- GAVRILENKO, G. M., GORSHKOV, A. P. and SCRIPKO, K. A., 1980 : Intensification of gas-hydrothermal activity of the Esmeralda submarine volcano in January 1978 and its influence on the chemical composition of seawater. Vulkanologiya i Seismologiya, No. 2, p. 19-29 (in Russian).
- GORSHKOV, A. P., ABRAMOV, V. A., SAPOZHNIKOV, E. A., SELIVERS-TOV, N. I. and RASHIDOV, V. A., 1980 : Geological structure of the Esmeralda submarine volcano. Vulkanologiya i Seismologiya, No. 4, p. 65-78 (in Russian).
- GORSHKOV, A. P., GREBZDY, E. I., SAMOILENKO, B. I. and SLEZIN, Yu. B., 1975 : On calculation of heat and mass balance of the Maly Semyachik crateric lake. Bull. Volc. St., No. 51, p. 50-59 (in Russian).
- GORSHKOV, A. P., and SLEZIN, Yu. B., 1972 : Thermal capacity and state of Zhupanovsky volcano in 1970. Bull. Volc. St., No. 48, p. 29-32 (in Russian).
- HESS, H. H., 1948 : Major structural features of the Western North Pacific, an interpretation of H.D. 5486, bathymetric chart, Korea to New Guinea. Bull. Geol. Soc. Amer., v. 59, No. 5, p. 417-445.
- KIRSANOVA, T. P. and ROZHKOV, A. M., 1975 : Heat flow in the Novy crater of Shiveluch volcano. Bull. Volc. St., No. 51, p. 60-63 (in Russian).

- KUNO, H., 1962 : Submarine volcano southwest of Saipan (8, 4-21). Catalogue of the active volcanoes and solfatara fields, part XI. Japan, Taiwan and Marianas. Roma-Napoli, p. 278.
- LAVROV, V. M., 1966 : Submarine volcanism of the Azores group of mountains in the northern Atlantic. In : Recent Volcanism. Proc. II All-Union Volc. Conf., 3-17 September, 1964, Moscow, v. 1, p. 24-32 (in Russian).
- POLYAK, B. G., 1966 : Geothermal peculiarities of the area of recent volcanism (as observed in Kamchatka), Moscow, Nauka, 180 pp. (in Russian).
- SIMONOVSKY, I. S. and KAMINSKY, B. D., 1975 : Interpretation of gravity and magnetic anomalies of vertical rotation bodies (direct task). In : Geophysical Methods of Prospecting in the Arctic. Leningrad, No. 10, p. 82-83 (in Russian).
- SINYUKOV, V. V., 1964 : On the influence of volcanic eruptions on the chemistry of ocean waters. Okeanologiya, v. 4, No. 4, p. 644-650 (in Russian).
- SUWA, A., 1965 : Japan (Description of volcanic eruptions). Bull. Volcan. Erup., No. 5, p. 4-5.
- SUWA, A. and OHURA, E., 1975 : Submarine volcano (Hukuzin-okanoba). Bull. Volcan. Erup., No. 13, p. 46-47.
- TANAKADATE, H., 1940 : Volcanoes in Mariana Islands in the Japanese Mandated South Seas. Bull. Volcanol. Ser. II, T. VI, p. 199-226.

A NEW CASE HISTORY  
OF GEOTHERMAL EXPLORATION  
IN VOLCANIC AREAS : THE LATERA FIELD  
(NORTHERN LATIUM, ITALY)

by

\* R. CATALDI, \* G. C. FERRARA,

\*\* R. FUNICELLO, and \* F. LOVARI

\*\* Istituto di Geologia

Università di Roma, Roma 00100

\* ENEL-UNG

Piazza Bartolo da Sassoferrato, Pisa 56100  
Italia

ABSTRACT

A new geothermal field, of the water-dominated type, has recently been discovered near the western border of the Monti Volsini volcanic region, in correspondence to a young caldera (0.2 m.y.). This caldera is marked by a subcircular gravimetric minimum which interrupts a N-S elongated positive anomaly characterizing a horst-like block of the sedimentary substratum.

This substratum underlies a more or less thin blanket of volcanics and is made up (from the top down) of : i) allochthonous flysch-facies units ; ii) a mainly carbonate complex locally referred to as the « Tuscan nappe » ; and iii) a schistose-quartzitic basement.

A magmatic body of syenitic composition intruded the lower part of the sedimentary substratum during the middle Pleistocene and a series of sills, originating from the main body, emplaced within the carbonate complex. The intrusion of the main body was probably controlled by the structural situation of the horst-like block, whereas the emplacement of the sills was apparently favoured by intersections of NS- and NE- trending fractures.

Some of these fractures were later sealed locally as a result of the skarn-like mineralization (epidote, almandine, K-feldspar, etc.) induced by the intrusive body and the associated sills.

The recent magmatic activity in the Latera area accounts for the high thermal anomaly (gradient values of up to  $2.5^{\circ}\text{C}/10\text{ m}$  and heat flow values of up to  $7\text{--}8\ \mu\text{cal}/\text{cm}^2\text{ sec}$  determined by geothermal prospecting), whereas the flysch-facies units and the underlying carbonate complex act as the impermeable cover and reservoir of the geothermal field, respectively.

This paper makes a further contribution to the study of geothermal «case histories»; after illustrating the methodology adopted to discover this field, it presents and briefly discusses the results of the two wells drilled so far in the Latera area.

The first well ( $> 340^{\circ}\text{C}$  at 2,900 m) is unproductive: the second well is, on the contrary, very productive, despite its lower temperature ( $\sim 210^{\circ}\text{C}$  at 1,400 m).

*(This paper was not read at the Symposium)*

# NEW INVESTIGATIONS ON THERMAL MANIFESTATIONS OF S. MIGUEL (AZORES)

by

A. BENCINI, M. MARTINI

Inst. of Mineralogy, Petrography and Geochemistry  
and G. PICCARDI

Inst. of Analytical Chemistry  
University of Florence (Italy)

The scientific interest for the thermal manifestations of S. Miguel dates back to Fouqué, whose results were published in 1873, while further contributions were given by Lepierre (1912) and Herculano de Carvalho (1953).

In 1969 Quintino in his study on the hydrothermal system of Furnas stressed the importance of the chemical analyses of the fumaroles and the thermal waters as an investigation tool in determining the characteristics of subsoil fluid circulation.

Apart from the more important researches carried out by the S. Miguel geothermal project, this paper is aimed to give a short up-to-date contribution on the basis of some chemical data obtained by surface sampling of fumaroles and thermal springs from Furnas and Agua de Pau areas.

Figure 1 shows the locations of the studied manifestations, which include also some cold waters.

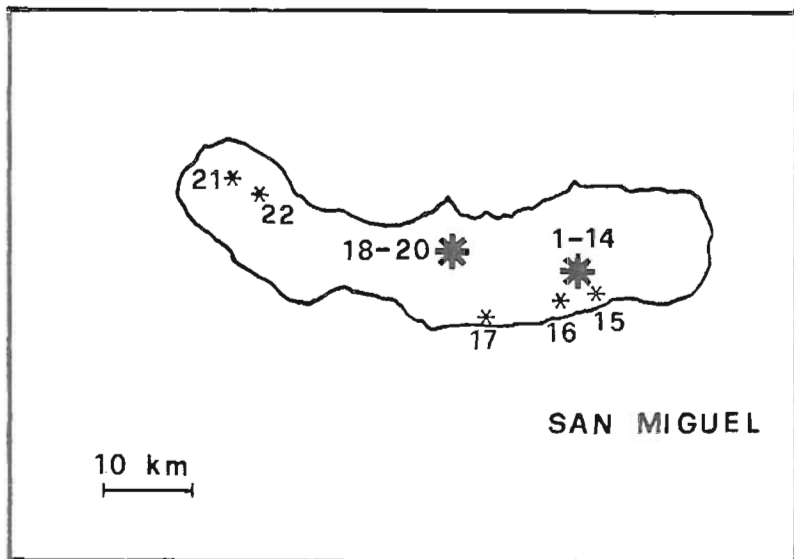


Figure 1 — Locations of the studied manifestations.

Table Ia and Ib give the analytical data for the waters.

The square diagram of fig. 2 allows to distinguish two different families, by the chemical standpoint, of bicarbonate and sulphate waters.

In considering the waters of bicarbonate composition it is easy to observe (fig. 3) that their pH values, ranging from 5.16 to 7.78, are correlated with the temperature. The weak acidity of these waters appears due to the greater solubility of carbon dioxide at lower temperatures.

Instead, the stronger acidity of sulphate waters is probably the result of surface oxidization of sulphur species, which allows a higher degree of rock alteration.

By a simple statistical cluster analysis it is possible to depict the fundamental associations between the investigated chemical characters (fig. 4). The resulting two main branches

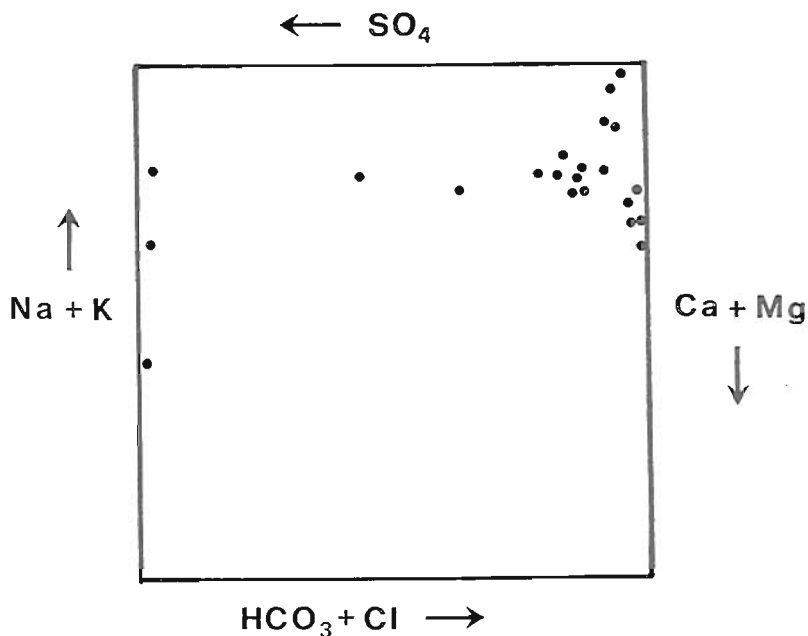


Figure 2—Square diagram representing the fundamental chemical composition.

point out the preferential grouping of chemical quantities which can correspond to different chemical processes, possibly giving rise to the observed different hydrochemical types.

In other words, the variables of the right branch should correspond to leaching of rocks by weakly acid hydrogencarbonate waters, giving rise to the bicarbonate type, while the other parameters should pertain to a stronger alteration process in acid environment, with resulting sulphate solutions.

The temperature was not considered by this statistical procedure since the surface measurements could give values not completely reliable.

Geothermometers based on concentrations of specific chemical indicators give sometimes deceiving information; in our

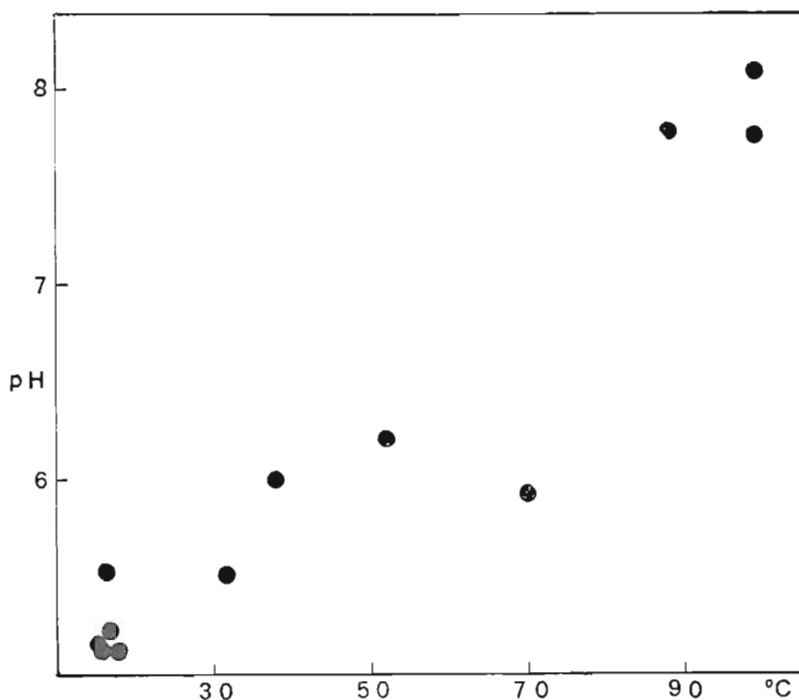


Figure 3 — Correlation between temperature and pH values of waters of bicarbonate type.

case, either the  $\text{SiO}_2$  or the Na/K geothermometer, if applied to the samples 9 and 10 with the highest temperatures and possibly the least affected by superficial changes, give values around  $100^\circ\text{C}$ .

The observed temperature of the first confined aquifer encountered by a drilling in Agua de Pau area at a depth of about 150 m is around  $110^\circ\text{C}$ ; since the inference of a similar hydrogeological pattern for the area of Furnas does not seem unreasonable, we can assume the calculated temperature as representative of a shallow confined aquifer.



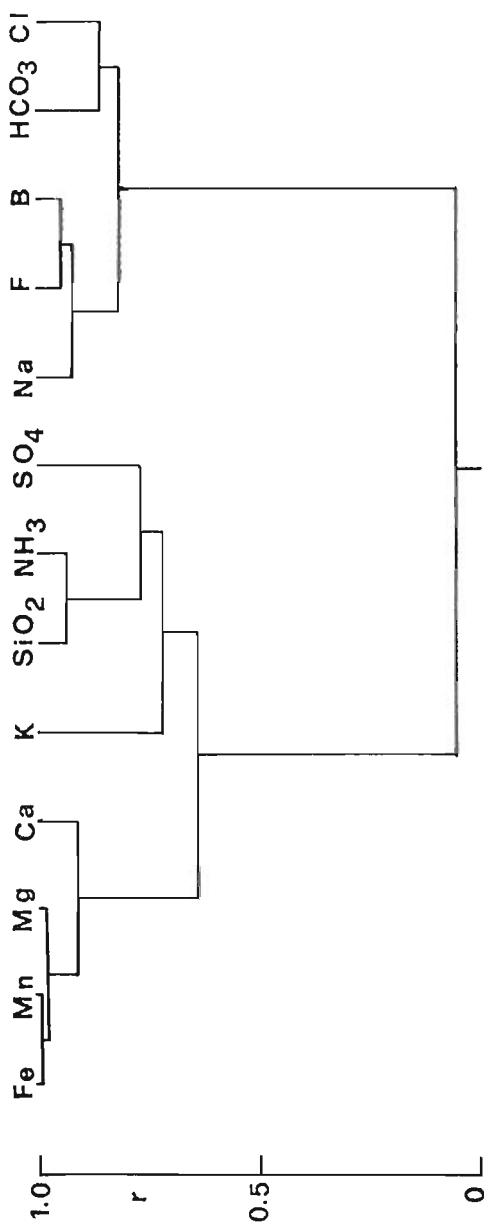


Figure 4 — Dendrogram resulting from a statistical cluster analysis of the chemical constituents.

The same calculating procedure cannot be safely applied for the other samples because :

- a) the acid waters of sulphate type presumably reflect a non-equilibrium situation of present alteration of rocks, yet not fulfilling a main condition of geothermometry ;

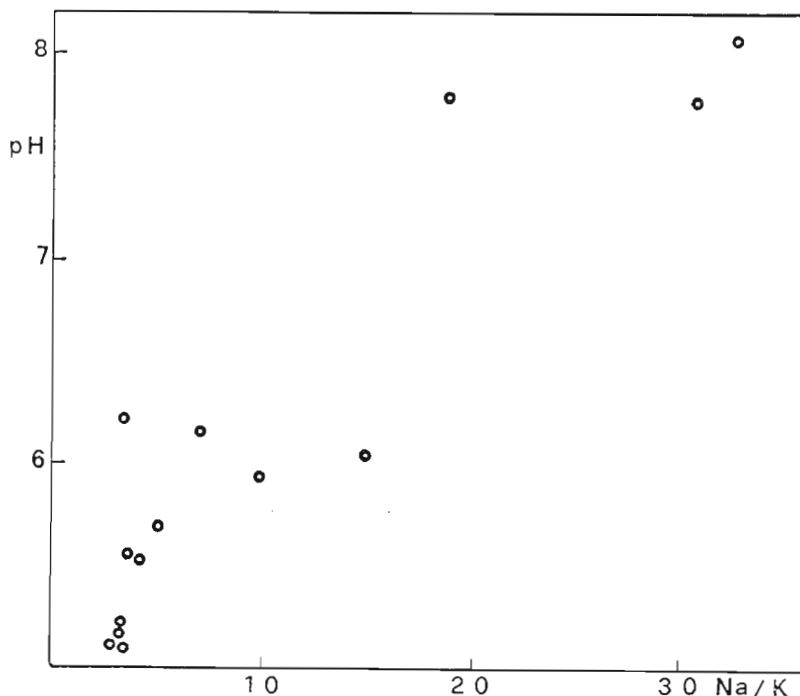


Figure 5 — Correlation between Na/K ratios and pH values of waters of bicarbonate type.

- b) the remaining waters of bicarbonate type show Na/K ratios depending on pH values (fig. 5) ; this can be ascribed to different degrees of leaching of rocks, with enrichment of K with respect to Na, due to the above

mentioned greater solubility of carbon dioxide in deep waters cooled by mixing with surface solutions; the again resulting non-equilibrium situation prevents any correct geothermometry.

The sodium bicarbonate waters appear to represent the shallow boiling aquifer outflowing in the low areas of Caldeiras das Furnas and Ribeira Quente. Samples 9 and 10 seem to keep better the original chemical-physical characters, while all the other samples pertaining to this group are the result of different degrees of dilution by surface waters.

At higher elevation this boiling aquifer is confined, but possible fractures can allow the escaping gases to reach the surface; their condensation gives rise to acid solutions, with increased degree of alteration of rocks and the observed change in chemical character. The surface acid waters are to be considered as an evidence of the deeper confined boiling aquifer.

Keeping into account the trace elements distribution, the ratio  $\text{NH}_4/\text{Li}$  seems well apt to discriminate between the two outlined genetic processes; while both lithium and ammonia can be present in the boiling aquifer, ammonia only is allowed to migrate upwards in the gaseous form. The observed values of the  $\text{NH}_4/\text{Li}$  ratio in the investigated samples fit rather well this hypothesis.

With reference to the main composition of the bubbling gases, the data from Caldeira de Esguicho and Ribeira Grande manifestations (table II) respectively of bicarbonate and sulphate type, point out a higher ratio of gas to water in the second kind of waters, again strenghtening the previous assumptions.

A systematic survey of chemical composition of ground waters, with special reference to the elements whose mobility can be to a large extent influenced by changes in the chemical-physical conditions of the subsoil environment, besides its importance for geothermal purposes, can act as a simple but effective tool in surveillance of active or potentially active volcanic areas.

Obviously, the chemical changes of ground waters cannot reflect short-time variations of the actual thermodynamic conditions, but can provide an integrated picture of some major trends in compositional characters well in advance of the establishing of critical conditions, thus allowing a long-term forecast.

Although the experiences on this subject are few and very recent, the usefulness of such a simple tool should not be underevaluated.

## REFERENCES

- CASTELO BRANCO, A., ZBYSZEWSKY, G., MEDEIROS, A. C. and ALMEIDA, F. M. (1957) : Etude géologique de la region de Furnas dans l'île de S. Miguel (Açores). Lisboa.
- FOUQUE, F. (1873) : Les eaux thermales de l'île de S. Miguel (Açores). Lisboa.
- HERCULANO DE CARVALHO, A. (1955) : Estudos analíticos de águas termais. (Direcção Geral de Minas e Serviços Geológicos, Lisboa).
- LEPIERRE, C. (1917) : Análise das águas minero-medicinais do vale das Furnas. Ilha de S. Miguel, Lisboa.
- MARTINI, M. and CELLINI LEGITTIMO, P. (1977) : Sul contenuto di ammonio in acque termali. Rend. Soc. It. Min. Petr., 33, p. 781-790.
- MUECKE, G. K., ADE-HALL, J. M., AUMENTO, F. MACDONALD A., REYNOLDS, P. H., HYNDMAN, R. D., QUINTINO, J., OPDYKE, N. and MOWRIE, W. (1974) : Deep drilling in an active geothermal area in the Azores. Nature, 252, p. 281-284.
- QUINTINO, J. (1969) : Sistemas hidrotermais associados ao vulcanismo e sua prospecção com fins económicos. Aplicação à região das Furnas (S. Miguel — Açores). Técnica, Lisboa.
- Progetto Finalizzato Geodinamica*, Publ. no. 334
- CNR Centro di Studio per la Mineralogia e la Geochimica dei Sedimenti.

TABLE Ia

Number	Sample location	Temp.	pH	Cond.	Ca	Mg	Na	K	HCO <sub>3</sub>	SO <sub>4</sub>	Cl
1	Lagoa das Furnas	78	2.81	1.8	4.6	4.5	5.6	.98	—	.23	.15
2	Lagoa das Furnas	15	5.59	.16	.25	.22	1.2	.24	1.3	.06	.41
3	Lagoa das Furnas	20	7.02	.13	.17	.18	.86	.19	.69	.61	.35
4	Prata	32	5.51	.32	.60	.30	2.2	.53	2.8	.47	.40
5	Miguel Henrique	16	5.52	.28	.43	.20	2.1	.56	2.2	.51	.49
6	Água Santa	88	7.78	.81	.22	.05	9.8	.52	6.7	.35	1.4
7	Caldeirão	70	5.93	.44	.46	.29	4.2	.41	4.0	.51	1.1
8	Rebentão	15	5.16	.23	.55	.33	1.5	.48	1.8	.35	.48
9	Caldeira de Esguicho	99	7.77	1.4	.17	.02	17	.55	9.6	1.3	6.3
10	Caldeira Grande	99	8.06	1.8	.19	.02	22	.64	12	1.6	8.2
11	Doutor Dimis	16	5.11	.26	.37	.28	1.6	.49	1.8	.36	.45
12	Chalet Frio	16	5.20	.28	.42	.28	1.7	.55	1.8	.60	.50
13	Água Azeda	15	5.13	.27	.37	.31	1.6	.53	1.9	.38	.43
14	Caldeira dos Vimes	56	6.23	.35	.45	.33	2.1	.63	1.2	2.1	.42
15	Ribeira Quente	38	6.03	1.2	2.8	1.2	11	.73	7.8	1.4	6.2
16	road to Furnas	14	7.73	.20	.30	.23	1.7	.15	1.0	.46	1.1
17	Água de Pau	16	7.68	.12	.19	.15	.91	.13	.64	.05	.58
18	Ribeira Grande	87	2.38	3.0	.95	.63	2.2	.70	—	16	.60
19	Ribeira Grande	17	6.16	.11	.10	.15	.83	.12	.86	.01	.52
20	Caldeira Velha	87	2.90	1.2	.32	.40	1.9	.78	—	8.0	.24
21	Lagoa das Sete Cidades	24	7.40	.09	.17	.11	.64	.06	.39	.05	.42
22	Canário	15	7.11	.14	.22	.28	.91	.16	1.0	0.2	.44

Table Ia — Fundamental chemical composition of the studied waters.  
 Values are expressed as milliequivalents per liter; specific conductivity is given in millimhos.

TABLE 1b

SYMPOSIUM ON THE ACTIVITY OF OCEANIC VOLCANOES

<i>Number</i>	<i>SiO<sub>2</sub></i>	<i>B</i>	<i>F</i>	<i>Li</i>	<i>NH<sub>4</sub></i>	<i>Sr</i>	<i>Fe</i>	<i>Mn</i>
1	7.0	.001	.23	.001	.55	.018	3.6	.23
2	1.2	.001	.047	.001	.012	.018	—	—
3	.50	.001	.046	.001	.030	.018	.007	.003
4	2.1	.001	.11	.003	.016	.023	.22	.021
5	1.7	.001	.12	.002	.005	.023	.066	.017
6	2.3	.49	.34	.018	.052	.001	—	.002
7	3.0	.16	.12	.007	.021	.025	.033	.021
8	1.9	.015	.13	.001	.012	.001	.20	.014
9	2.1	1.1	.70	.035	.018	.028	—	.001
10	2.2	1.4	.92	.045	.043	.001	—	—
11	1.9	.001	.052	.001	.042	.001	.065	.012
12	1.8	.020	.050	.001	.069	.001	.017	.018
13	1.8	.001	.050	.001	.050	.001	.076	.018
14	1.5	.001	.067	.001	.066	.001	.010	.014
15	2.8	.066	.25	0.18	.009	.037	.25	.034
16	1.1	.020	.059	.001	.007	.001	—	—
17	1.0	.030	.038	.001	.005	.001	—	.019
18	4.6	.046	.24	.002	.13	.028	.57	.022
19	1.2	.002	.050	.001	.004	.005	—	—
20	8.0	.066	.20	.003	.62	.021	.53	.033
21	.001	.001	.024	.001	.037	.003	—	—
22	.90	.001	.016	.001	.035	.001	—	—

Table 1b — Concentrations of minor constituents in the studied samples.

Values are expressed as milliequivalents per liter for F, Li, NH<sub>4</sub>, Sr, Fe, Mn, and as millimoles per liter for SiO<sub>2</sub> and B.

TABLE II

	$H_2O$	$CO_2$	$H_2S$	<i>gas/water</i> <i>lt/kg</i>
Caldeira de Esguicho	92.8	7.1	0.03	96
Ribeira Grande	81.1	18.7	0.02	289

Table II — Volume percentage composition of the bubbling gases.